Equation of state of neutron star matter, and the nuclear symmetry energy

Doan Thi Loan,[1] Ngo Hai Tan,[1] Dao T. Khoa,[1,*] and Jerome Margueron[2]
[1]*Institute for Nuclear Science and Technique, VAEC, 179 Hoang Quoc Viet Road, Nghia Do, Hanoi, Vietnam*
[2]*Institut de Physique Nucléaire, IN2P3-CNRS/Université Paris-Sud, F-91406 Orsay, France*
(Received 31 March 2011; revised manuscript received 13 May 2011; published 27 June 2011)

The nuclear mean-field potentials obtained in the Hartree-Fock method with different choices of the in-medium nucleon-nucleon (NN) interaction have been used to study the equation of state (EOS) of the neutron star (NS) matter. The EOS of the uniform NS core has been calculated for the $npe\mu$ composition in the β equilibrium at zero temperature, using version Sly4 of the Skyrme interaction as well as two density-dependent versions of the finite-range M3Y interaction (CDM3Y*n* and M3Y-P*n*), and versions D1S and D1N of the Gogny interaction. Although the considered effective NN interactions were proven to be quite realistic in numerous nuclear structure and/or reaction studies, they give quite different behaviors of the symmetry energy of nuclear matter at supranuclear densities that lead to the *soft* and *stiff* scenarios discussed recently in the literature. Different EOS's of the NS core and the EOS of the NS crust given by the compressible liquid drop model have been used as input of the Tolman-Oppenheimer-Volkov equations to study how the nuclear symmetry energy affects the model prediction of different NS properties, like the cooling process as well as the gravitational mass, radius, and moment of inertia.

DOI: 10.1103/PhysRevC.83.065809 PACS number(s): 26.60.Kp, 21.65.Cd, 21.65.Ef, 26.60.Dd

I. INTRODUCTION

The determination of the equation of state (EOS) of asymmetric nuclear matter (NM) has been the main object of numerous nuclear structure and reaction studies involving unstable nuclei lying close to the neutron or proton driplines [1]. The knowledge about the EOS of asymmetric NM is vital for any model of neutron star [2–7], and the nuclear mean-field potential is the most important input for the determination of the nuclear EOS. Many microscopic studies of the EOS have been done based on the nuclear mean field given by both nonrelativistic and relativistic nuclear many-body approaches, using realistic two-body and three-body nucleon-nucleon (NN) forces or interaction Lagrangians (see recent reviews in Refs. [1,8]). These many-body studies have shown the important role played by the Pauli blocking effects as well as higher-order NN correlations at different NM densities. These medium effects are normally considered as the physics origin of the density dependence that has been introduced into various versions of the effective NN interactions used in the modern mean-field approaches. Among them, very popular is the so-called M3Y interaction, which was originally constructed to reproduce the G-matrix elements of the Reid [9] and Paris [10] NN potentials in an oscillator basis. Several realistic density dependences were added later on to the M3Y interactions [11–16] to properly account for the NM saturation properties as well as the ground-state structure of finite nuclei [17–19]. These density-dependent versions of the M3Y interaction were used in the nonrelativistic Hartree-Fock (HF) studies of symmetric and asymmetric NM. Some of them were successfully used in the folding model studies of the nucleon-nucleus and nucleus-nucleus scattering [13–15,20–22].

In an attempt to find a realistic version of the effective NN interaction for consistent use in the mean-field studies of NM and finite nuclei as well as in the nuclear reaction calculations, we performed recently a systematic HF study of NM [23] using the CDM3Y*n* interactions, which have been used mainly in the folding model studies of the nuclear scattering [14,15,21,22], and the M3Y-P*n* interactions carefully parametrized by Nakada [17–19] for use in the HF studies of nuclear structure. For comparison, the same HF study has also been done with the D1S and D1N versions of the Gogny interaction [24,25] and Sly4 version of the Skyrme interaction [26]. While these effective NN interactions give more or less the same description of the saturation properties of the symmetric NM, the HF results for the asymmetric NM [23] show that they are divided into two families, which are associated with two different (*soft* and *stiff*) behaviors of the NM symmetry energy at high nucleon densities. As a result, these two families predict very different behaviors of the proton-to-neutron ratio in the β equilibrium that can imply two drastically different mechanisms for the neutron star cooling (with or without the direct Urca process) [27–29].

As a further step in this direction, we try to find out in the present work how such a difference in the NM symmetry energy can affect the EOS of the β-stable neutron star (NS) matter as well as the main NS properties like the maximum mass, radius, central density, and moment of inertia. For this purpose, the Tolman-Oppenheimer-Volkov (TOV) equations have been solved using different EOS's of the NS matter that are associated with the nuclear mean-field potentials given by the different in-medium NN interactions under study. Given the complex, inhomogeneous structure of the NS crust, it is a tremendous task to develop a consistent structure model for the inner and outer NS crusts using all versions of the in-medium NN interaction considered here. Therefore, we have used the EOS of the NS crust given by the compressible liquid drop model (CLDM) [5,30] with the model parameters determined

*Corresponding author: khoa@vaec.gov.vn

by the SLy4 interaction [26]. Different EOS's of the uniform NS core are then calculated for the $npe\mu$ composition in the β equilibrium at zero temperature and extended to the supranuclear densities, using the mean-field potentials given by different density-dependent NN interactions. In this way, any difference found in the solutions of the TOV equations is entirely due to the choice of the EOS of the NS core (i.e., to the choice of the in-medium NN interaction). The main NS properties obtained in each case are compared with the empirical data given by the recent astronomical observation of neutron stars.

II. HARTREE-FOCK CALCULATION OF ASYMMETRIC NUCLEAR MATTER

We recall here the main features of our HF study [23] of the uniform (spin-saturated) NM at zero temperature that is characterized by given values of the neutron and proton densities n_n and n_p, or equivalently by the total density $n_b = n_n + n_p$ (hereafter referred to as the baryon density) and the neutron-proton asymmetry $\delta = (n_n - n_p)/(n_n + n_p)$. With the direct ($v_D$) and exchange ($v_{\rm EX}$) parts of the interaction determined from the singlet- and triplet-even (and odd) components of the central NN force, the total energy density of the NM is determined as

$$\varepsilon = \varepsilon_{\rm kin} + \frac{1}{2}\sum_{k\sigma\tau}\sum_{k'\sigma'\tau'}[\langle \boldsymbol{k}\sigma\tau, \boldsymbol{k}'\sigma'\tau'|v_D|\boldsymbol{k}\sigma\tau, \boldsymbol{k}'\sigma'\tau'\rangle + \langle \boldsymbol{k}\sigma\tau, \boldsymbol{k}'\sigma'\tau'|v_{\rm EX}|\boldsymbol{k}'\sigma\tau, \boldsymbol{k}\sigma'\tau'\rangle], \quad (1)$$

where $|\boldsymbol{k}\sigma\tau\rangle$ are the ordinary plane waves. Dividing ε over the total baryon number density n_b, we obtain the total NM energy per particle E that can be expressed as

$$\frac{\varepsilon}{n_b} \equiv E(n_b, \delta) = E(n_b, \delta = 0) + S(n_b)\delta^2 + O(\delta^4) + \cdots . \quad (2)$$

The NM pressure P and incompressibility K are then calculated as

$$P(n_b, \delta) = n_b^2 \frac{\partial E(n_b, \delta)}{\partial n_b}, \qquad K(n_b, \delta) = 9n_b^2 \frac{\partial^2 E(n_b, \delta)}{\partial n_b^2}. \quad (3)$$

The contribution of $O(\delta^4)$ and higher-order terms in Eq. (2) was proven to be quite small [13,31] and is often neglected in the so-called *parabolic* approximation, where the NM *symmetry energy* $S(n_b)$ equals the energy required per particle to change the symmetric NM into the pure neutron matter. The value of $S(n_b)$ at the symmetric NM saturation density $n_0 \approx 0.17$ fm^{-3} is known as the symmetry energy coefficient $J = S(n_0)$ that was predicted by numerous many-body calculations to be around 30 MeV [13,31–33].

The knowledge about the density dependence of $S(n_b)$ is extremely important for the construction of nuclear EOS and it has been, therefore, a longstanding goal of many nuclear structure and reaction studies. The main method to probe $S(n_b)$ associated with a given in-medium NN interaction is to test this interaction in the simulation of heavy-ion (HI) collisions using transport and/or statistical models [1,34–40] or in the structure studies of nuclei with large neutron excess [19,25,26,41–49]. Based on the physics constraints implied by such studies, an extrapolation is often made to draw a conclusion on the low- and high-density behavior of $S(n_b)$. However, such conclusions still remain quite divergent in some cases [23]. One of the most intriguing issues discussed recently in the literature is whether the "soft" or "stiff" density dependence of the NM symmetry energy is more realistic. These two scenarios are well illustrated in Fig. 1 where the HF results obtained with the two groups of the considered in-medium NN interactions are plotted.

For comparison, we have also plotted in Fig. 1 the results of the *ab initio* variational chain-summation calculation using the A18 + δv + UIX* version of the Argonne NN potential by Akmal, Pandharipande, and Ravenhall (APR) [50] and recent microscopic Monte Carlo calculation of neutron star structure by Gandolfi *et al.* [51], using the Argonne AV6′ potential added by an empirical density dependence.

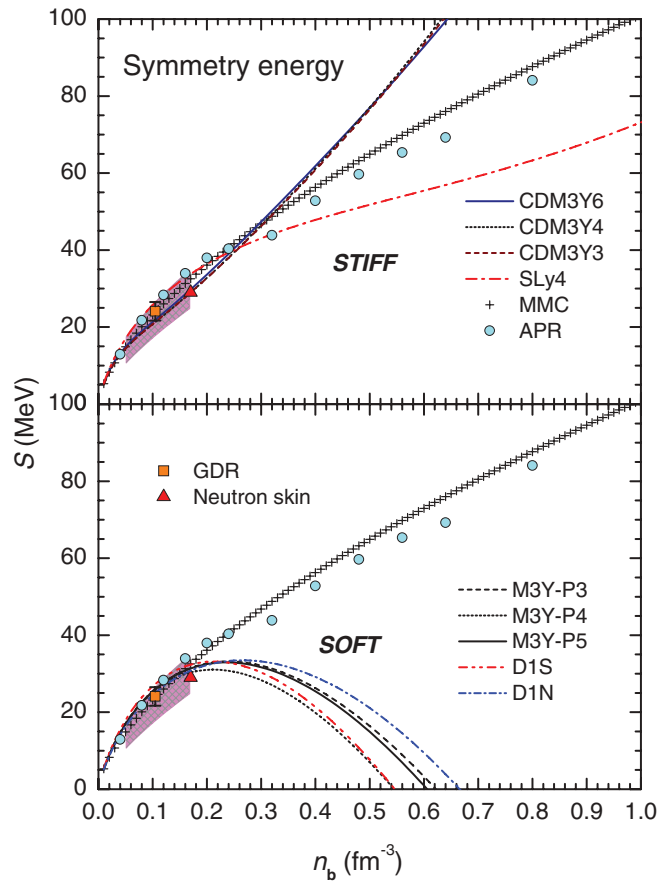

FIG. 1. (Color online) HF results for the NM symmetry energies $S(n_b)$ given by the density-dependent NN interactions under study. The shaded (magenta) region marks the empirical boundaries deduced from the analysis of the isospin diffusion data and double ratio of neutron and proton spectra data of HI collisions [34,36]. The square and triangle are the constraints deduced from the consistent structure studies of the GDR [47] and neutron skin [49], respectively. The circles and crosses are results of the *ab initio* calculation by Akmal, Pandharipande, and Ravenhall (APR) [50] and microscopic Monte Carlo (MMC) calculation by Gandolfi *et al.* [51], respectively.

Around the saturation density n_0 of the symmetric NM all the models predict the symmetry coefficient $S(n_0) = J \approx 29 \pm 3$ MeV, in a reasonable agreement with the empirical values deduced recently from the structure studies of neutron skin [48,49]. In the low-density region ($n_b \approx 0.3 \sim 0.6\ n_0$) there exist empirical boundaries for the symmetry energy deduced from the analysis of the isospin diffusion data and double ratio of neutron and proton spectra data of HI collisions [34,36], which enclose the HF results given by both groups of the in-medium NN interactions. At the baryon density $n_b \approx 0.1$ fm^{-3}, all the HF results also agree quite well with the empirical value deduced from a consistent structure study of the isovector giant dipole resonance (GDR) in heavy nuclei [47]. So far there are no firm empirical constraints on the NM symmetry energy at supranuclear densities, and the behavior of $S(n_b)$ at high densities remains uncertain. The two different behaviors of $S(n_b)$ shown in Fig. 1 have been observed earlier [1,38,52,53] and often discussed in the literature as the *Asy-stiff* (with symmetry energy steadily increasing with density) and *Asy-soft* (with symmetry energy reaching saturation and then decreasing to negative values) behaviors. The main characteristics of the EOS's obtained with these two groups of density-dependent NN interactions have been discussed in detail in Ref. [23]. We note here that most of the microscopic calculations of NM like the *ab initio* APR results [50] or the Monte Carlo calculation by Gandolfi *et al.* [51] do predict a stiff behavior of the nuclear symmetry energy, excepting perhaps the microscopic study by Wiringa *et al.* [54] that predicted a soft behavior of $S(n_b)$ using the Argonne or Urbana NN interaction plus a three-nucleon interaction term. The stiff behavior is also predicted by the recent microscopic Brueckner-Hartree-Fock (BHF) or Dirac-Brueckner-Hartree-Fock calculations of NM that include the higher-order many-body correlations and/or three-body forces [7,55,56] as well as by the latest relativistic mean-field studies [42–44]. Because the isovector density dependence of the CDM3Yn interactions has been parametrized [15] to reproduce simultaneously the BHF results obtained by Jeukenne, Lejeune, and Mahaux [57] for the isospin and density dependent nucleon optical potential and the charge exchange (p, n) data for the isobaric analog excitation [15], the *stiff* behavior of $S(n_b)$ given by the CDM3Yn interactions is quite close to that given by the BHF calculation. If we simply assume the density dependence of the isovector part of CDM3Yn interactions to be the same as that of the isoscalar part, then $S(n_b)$ has a *soft* behavior that was discussed in our earlier HF study [13]. However, the isovector density dependence of the M3Y-Pn, D1S, and D1N interactions were carefully fine-tuned against the structure data observed for a wide range of the neutron (and proton) dripline nuclei and the low-density tail of $S(n_b)$ predicted by these interactions should be quite realistic. However, there is no physics ground to confirm the validity of the high-density behavior of $S(n_b)$ predicted by the *soft* M3Y-Pn, D1S, and D1N interactions. For the total NM energy (2) that is sometimes referred to as the nuclear EOS, the HF results given by all considered interactions for the symmetric NM agree well with the microscopic APR or Monte Carlo predictions. However, the difference in the symmetry energy lead to very different behaviors of the energy of pure neutron matter given by the stiff and soft groups of interactions (see the lower panels of Figs. 2 and 3). In terms of the NM pressure (3) the soft-type interactions have been shown [23] unable to reproduce the empirical pressure $P(n_b)$ of the pure neutron matter deduced from the HI flow data [35]. In the present work we make such a comparison more accurately based on the mean-field prediction for the EOS of the NS matter of the $npe\mu$ composition in the β equilibrium and the recent empirical data deduced from astrophysical measurements of neutron stars by Özel *et al.* [58] and Steiner *et al.* [59].

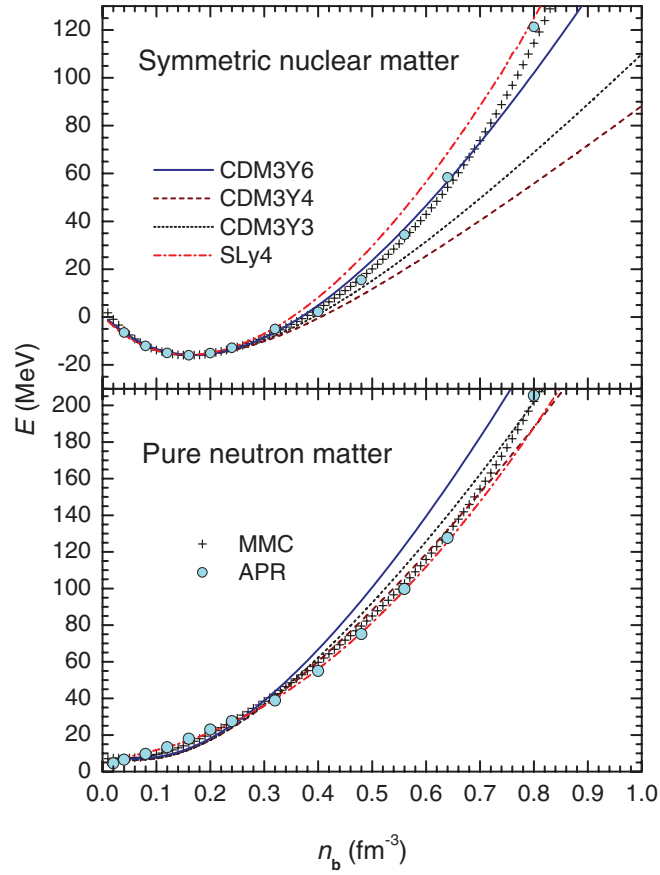

FIG. 2. (Color online) Energy of the symmetric NM and pure neutron matter calculated in the HF approximation (1) and (2) using the in-medium NN interactions that give a *stiff* behavior of $S(n_b)$ as shown in the upper panel of Fig. 1. The circles and crosses are results of the *ab initio* calculation by APR [50] and MMC calculation by Gandolfi *et al.* [51], respectively.

III. EOS OF THE β-STABLE NEUTRON STAR MATTER

Nuclei in the NS crust are described by the CLDM by Douchin *et al.* (see Ref. [30] and references therein), using the model parameters determined with the version SLy4 of the Skyrme interaction [26]. Within the CLDM, electrons inside the inhomogeneous NS crust are assumed to form a relativistic Fermi gas. The structure of the NS crust has been given by the CLDM for the baryon densities up to the *edge* density $n_{\rm edge} \approx 0.076$ fm^{-3}, where a weak first-order phase transition between the NS crust and liquid (uniform) core takes place [5].

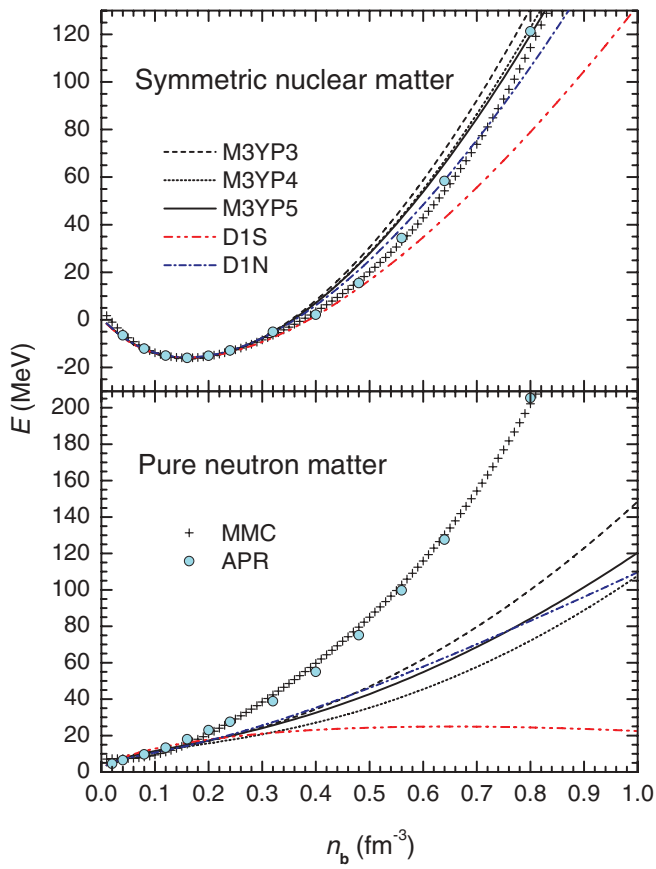

FIG. 3. (Color online) The same as Fig. 2 but obtained with the in-medium NN interactions that give a *soft* behavior of $S(n_b)$ as shown in the lower panel of Fig. 1.

At baryon densities $n_b > n_{\rm edge}$ the NS core is described as a homogeneous matter of neutrons, protons, electrons, and negative muons (μ^- appear at n_b above the muon threshold density, where the electron chemical potential $\mu_e > m_\mu c^2 \approx$ 105.6 MeV). Such a $npe\mu$ composition of the NS core is a realistic assumption up to the high densities of $n_b \simeq 3n_0$. Although the appearance of hyperons can be expected at higher densities, Douchin and Haensel have extrapolated their $npe\mu$ model for the EOS of the NS matter up to the maximum central density (the approach used earlier in the *ab initio* study by Akmal *et al.* [50]). Thus, the total energy density ε of the $npe\mu$ matter (including the rest energy of baryons and leptons) is determined in the present study as

$$\varepsilon(n_n, n_p, n_e, n_\mu) = \varepsilon_{\rm HF}(n_n, n_p) + n_n m_n c^2 + n_p m_p c^2 + \varepsilon_e(n_e) + \varepsilon_\mu(n_\mu), \quad (4)$$

where $\varepsilon_{\rm HF}(n_n, n_p)$ is the Hartree-Fock energy density of nucleons (1); ε_e and ε_μ are the energy densities of electrons and muons, respectively, which are evaluated in the relativistic Fermi gas model, neglecting electrostatic interaction [5,60]. The number densities of leptons n_e and n_μ are determined from the charge neutrality condition ($n_p = n_e + n_\mu$) and the relation for the chemical potentials, implied by the β equilibrium of the (neutrino-free) NS matter

$$\mu_n = \mu_p + \mu_e \text{ and } \mu_\mu = \mu_e, \quad \text{where } \mu_j = \frac{\partial \varepsilon}{\partial n_j}, \quad j = n, p, e, \mu. \quad (5)$$

As a result, we can determine uniquely all fractions of the constituent particles $x_j = n_j/n_b$ at the given baryon density $n_b = n_n + n_p$. Below the muon threshold density ($\mu_e < m_\mu c^2 \approx 105.6$ MeV) the charge neutrality condition leads to the following relation [60]

$$3\pi^2(\hbar c)^3 n_b x_p - \hat{\mu}^3 = 0, \quad \text{where } \hat{\mu} = \mu_n - \mu_p = 2\frac{\partial E}{\partial \delta}\Big|_{n_b}. \quad (6)$$

Using the total NM energy E given by the HF calculation (2), the density dependence of the proton fraction in the β equilibrium $x_p(n_b)$ is readily obtained from the solution of Eq. (6). If we assume the parabolic approximation and neglect the contribution from higher-order terms in Eq. (2), then $x_p(n_b)$ is given by the solution of the well-known equation [6]

$$3\pi^2(\hbar c)^3 n_b x_p - [4S(n_b)(1-2x_p)]^3 = 0, \quad (7)$$

which shows the crucial role of the NM symmetry energy in the determination of the proton abundance in the NS matter.

As the baryon density exceeds the muon threshold density, where $\mu_e > m_\mu c^2 \approx 105.6$ MeV, it is energetically favorable for electrons to convert to negative muons and the charge neutrality condition leads now to the relation [60]

$$3\pi^2(\hbar c)^3 n_b x_p - \hat{\mu}^3 - [\hat{\mu}^2 - (m_\mu c^2)^2]^{3/2}\theta(\hat{\mu} - m_\mu c^2) = 0, \quad (8)$$

where $\theta(x)$ is the Heaviside step function. Based on the solutions of Eqs. (6) and (8), the EOS of the $npe\mu$ matter is fully determined by the mass density $\rho(n_b)$ and total pressure $P(n_b)$ inside the neutron star

$$\rho(n_b) = \varepsilon(n_b)/c^2, \quad P(n_b) = n_b^2 \frac{\partial}{\partial n_b}\left[\frac{\varepsilon_{\rm HF}(n_b)}{n_b}\right] + P_e + P_\mu. \quad (9)$$

In the present study, we have first solved Eqs. (6) and (8) to determine all fractions $x_j = n_j/n_b$ and the EOS of the $npe\mu$ matter using the total baryon energy $E(n_b)$ given by the Sly4 interaction. The accuracy of the numerical procedure was double checked against the published results for $x_j(n_b)$ and $P(n_b)$, obtained with the Sly4 interaction by Douchin and Haensel (tabulated in Refs. [5,61]). Different EOS's of the NS core were then calculated for the $npe\mu$ matter, using the HF mean-field energies given by different in-medium NN interactions considered in our study.

Our results for the fractions $x_j = n_j/n_b$ obtained with different interactions are plotted in Figs. 4 and 5. For the typical soft-type interactions (like the results obtained for the M3Y-P5 and D1N interactions shown here), the proton and lepton fractions are quite small and reach their maxima of around 4% at $n_b \approx 0.2$ fm^{-3} (see the lower panels of Fig. 4), at exactly

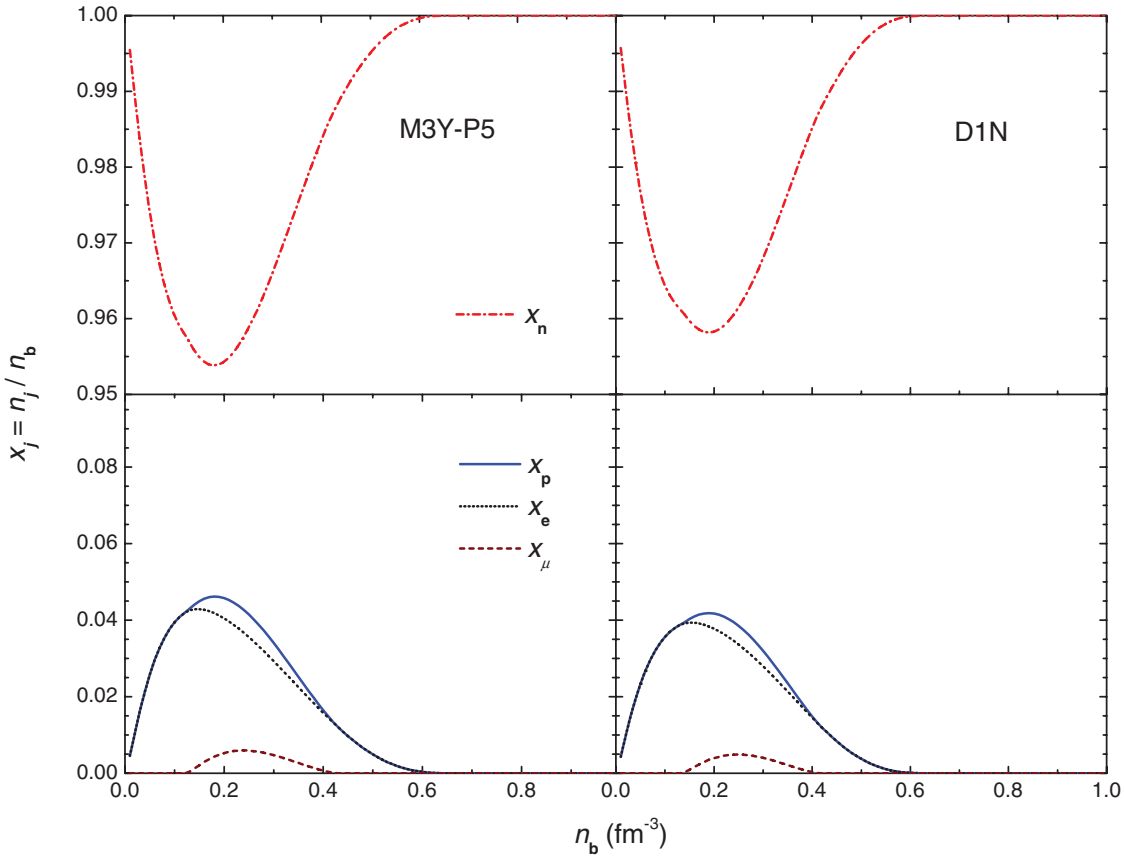

FIG. 4. (Color online) The fractions $x_j = n_j/n_b$ of constituent particles of the NS matter obtained from the solutions of Eqs. (6) and (8) using the mean-field potentials given by the M3Y-P5 and D1N interactions.

the same baryon density where the symmetry energy $S(n_b)$ goes through its maximum value. The fast decrease of $S(n_b)$ to zero at $n_b \approx 0.6 - 0.7$ fm^{-3} leads also to a drastic decrease of the proton and lepton components in the NS matter that then becomes β-*unstable*, pure neutron matter at $n_b > 0.6$ fm^{-3} (see the upper panels of Fig. 4).

The fractions $x_j = n_j/n_b$ obtained with the stiff-type interactions (see the results obtained for the CDM3Y4 and Sly4 interactions shown in Fig. 5) are substantially different from those given by the soft-type interactions. Namely, the proton and lepton fractions increase steadily with the baryon density like the corresponding symmetry energy $S(n_b)$. For the CDM3Yn interactions, the proton fraction x_p is above 30% at the maximum central density $n_c \approx 1.3$ fm^{-3}, and the matter at the NS center becomes less neutron rich (with $x_n < 70\%$). In this case, the β equilibrium of the charge neutral NS matter is kept throughout the NS core, with the lepton fractions reaching more than 30% at n_c (see the left-lower panel of Fig. 5). It is interesting to note that about the same behavior of x_p is also predicted by the recent complete EOS of nuclear matter by Shen *et al.* [62], constructed for use in astrophysical simulations. For the Sly4 interaction, with a less stiff increase of $S(n_b)$ at large densities (see the upper panel of Fig. 1), the maximum proton fraction at $n_c \approx 1.2$ fm^{-3} is only about 12% and the NS matter is therefore more neutron rich compared to the case of CDM3Yn interactions. Nevertheless, in the case of Sly4 interaction the NS matter remains always in the β equilibrium [5].

As already discussed in Ref. [23], the behavior of the density dependence of the proton fraction $x_p(n_b)$ plays a very important role in the determination of the NS cooling rate. In particular, the powerful direct Urca (DU) process of neutrino emission is allowed only if the Fermi momenta of the constituent particles in the $npe\mu$ matter satisfy the triangle conditions [27] that lead to the existence of a DU threshold $x_{\rm DU}$ for the proton fraction that can be estimated [7] as

$$x_{\rm DU} = \frac{1}{1 + \left(1 + r_e^{1/3}\right)^3}, \tag{10}$$

where $r_e = n_e/(n_e + n_\mu)$ is the leptonic electron fraction. $x_{\rm DU}$ has its lowest value of 11.1% at $r_e = 1$ that corresponds to the muon-free threshold for the DU process [28]. It can be concluded immediately from the lower panel of Fig. 4 that the DU process is *not* possible for the NS matter generated with the soft-type interactions when x_p can reach, at most, 4% and then decreases quickly to zero at $n_b > 0.6$ fm^{-3}. Such a (mean-field) challenge to the soft-type in-medium NN interactions has been pointed out and discussed in Ref. [23]. Figure 6 shows that for the stiff-type CDM3Yn interactions, the proton fraction becomes larger than the DU threshold at a rather modest threshold density of $n_b \approx 0.45$ fm^{-3} that is far

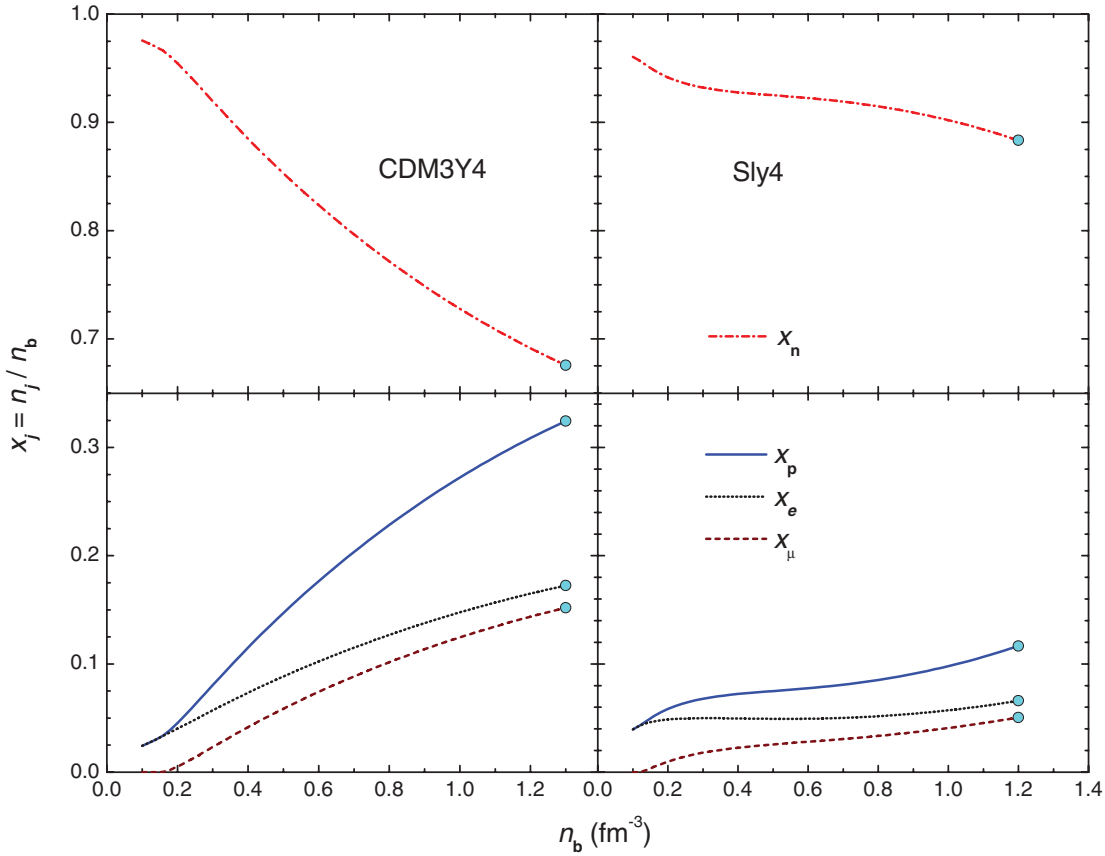

FIG. 5. (Color online) The same as Fig. 4 but using the mean-field potentials given by the CDM3Y4 and Sly4 interactions. The circles are n_j values calculated at the maximum central densities n_c given by the solution of the TOV equations.

below the corresponding maximum central densities of 1.2–1.3 fm^{-3}. Therefore, the DU process should be a realistic scenario for the NS cooling if the mean-field potential is generated with the CDM3Yn interactions. For the Sly4 interaction, the x_p value remains well below the DU threshold up to the maximum central density determined by the TOV equations and the DU process is thus not likely for the NS matter generated with the Sly4 interaction [5].

We discuss now our results obtained for the total pressure $P(n_b)$ inside the neutron star determined by relation (9), which defines the EOS of the NS matter to be used in the TOV equations. The NS pressure obtained with the HF mean-field energies $E(n_b)$ given by different in-medium NN interactions are plotted in Fig. 7. Since the lepton pressure $(P_e + P_\mu)$ inside the NS is about one order of magnitude weaker than the baryon pressure P_b, the results shown in Fig. 7 are determined predominantly by P_b. One of the main constraints for the NS matter is that the pressure must satisfy the relation $dP/dn \gtrsim 0$ to ensure the NS matter stability [63]. This (microscopic) stability condition also is known as le Chatelier's principle [60]. One can see in the lower panel of Fig. 7 that P obtained with the D1S version of the Gogny interaction does not comply with such a constraint and this interaction should not be used to generate the EOS of the NS matter at densities $n_b \gtrsim 2n_0$. This result stresses again that there can be a plethora of systematic uncertainties in different models of the in-medium NN interaction that are not visible at low nuclear densities, and the success of any interaction in the nuclear structure study is not sufficient to ensure its extrapolation to supranuclear densities.

With the advance in both the astrophysical techniques and modeling of the NS structure, it became recently feasible to empirically deduce the pressure of the NS matter at supranuclear densities [58]. The empirical pressure determined from the masses and radii observed for the binaries 4U 1608-248, EXO 1745-248, and 4U 1820-30 are plotted in Fig. 7 as the three data points spanned by a shadow region of the uncertainties associated with the data determination [58]. From Fig. 7 one can see that both groups of in-medium NN interaction agree more or less with the data for NS pressure, while a similar comparison [23] of the pressure calculated for pure neutron matter with the empirical value deduced from the HI flow data [35] seemed to favor the stiff-type interactions. To distinguish more clearly the EOS's given by these two groups of interactions, we have further used them in the input of the TOV equations to study the main NS properties.

IV. NEUTRON STAR PROPERTIES

Different sets of predicted mass density ρ and total pressure P inside the neutron star (9) have been further used to solve

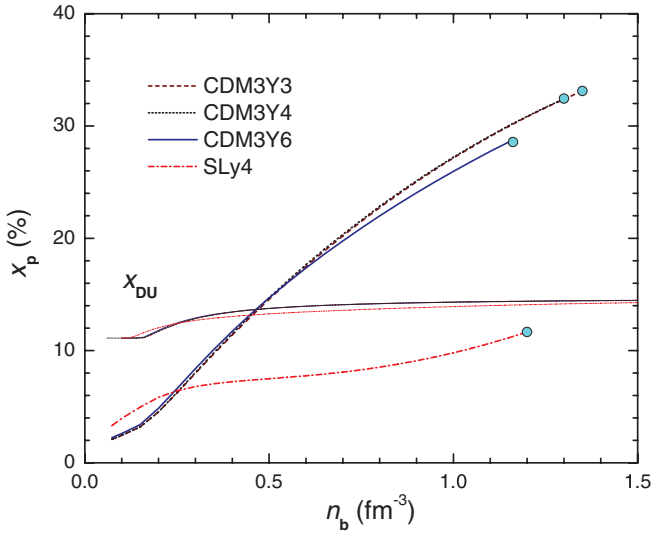

FIG. 6. (Color online) The proton fraction x_p of the β-stable NS matter obtained from the solutions of Eqs. (6) and (8) using the mean-field potentials given by the stiff-type CDM3Yn and Sly4 interactions. The circles are n_p values calculated at the maximum central densities n_c given by the TOV equations. The thin lines are the corresponding DU thresholds (10).

the well-known TOV equations

$$\frac{dP}{dr} = -G\frac{m\rho}{r^2}\left(1+\frac{P}{\rho c^2}\right)\left(1+\frac{4\pi Pr^3}{mc^2}\right)\left(1-\frac{2Gm}{rc^2}\right)^{-1},$$
$$\frac{dm}{dr} = 4\pi r^2\rho, \qquad (11)$$

where G is the universal gravitational constant, r is the radial coordinate in the Schwarzschild metric, and m is the gravitational mass enclosed within the sphere of radius r. The TOV equations (11) are supplemented with the following equation determining the number of baryons a inside this sphere [5]

$$\frac{da}{dr} = 4\pi r^2 n_b\left(1-\frac{2Gm}{rc^2}\right)^{-1/2}. \qquad (12)$$

Equations (11) and (12) have been integrated from the NS center, with the boundary conditions at $r = 0$: $P(0) = P_c$, $m(0) = 0$, $\rho(0) = \rho_c$, and $a(0) = 0$. The stellar surface at $r = R$ is determined from the boundary condition $P(R) = 0$. The total gravitational mass and total number of baryons are then determined as $M = m(R)$, $A = a(R)$, respectively. As a result, with different inputs for the NM pressure, the corresponding solutions of the TOV equations give different NS models in terms of *one-parameter* families [5] that can be labeled by the central pressure P_c or equivalently by the central density ρ_c of the neutron star.

Thus, at each central density we can uniquely determine the corresponding gravitational mass M and radius R, and the behavior of M versus R is often used to compare with the measured masses and radii of neutron stars. Our results obtained with different EOS's are plotted in Fig. 8. The recently measured masses and radii for the binaries 4U 1608-248, EXO 1745-248, and 4U 1820-30 [58] are plotted in Fig. 8 as the

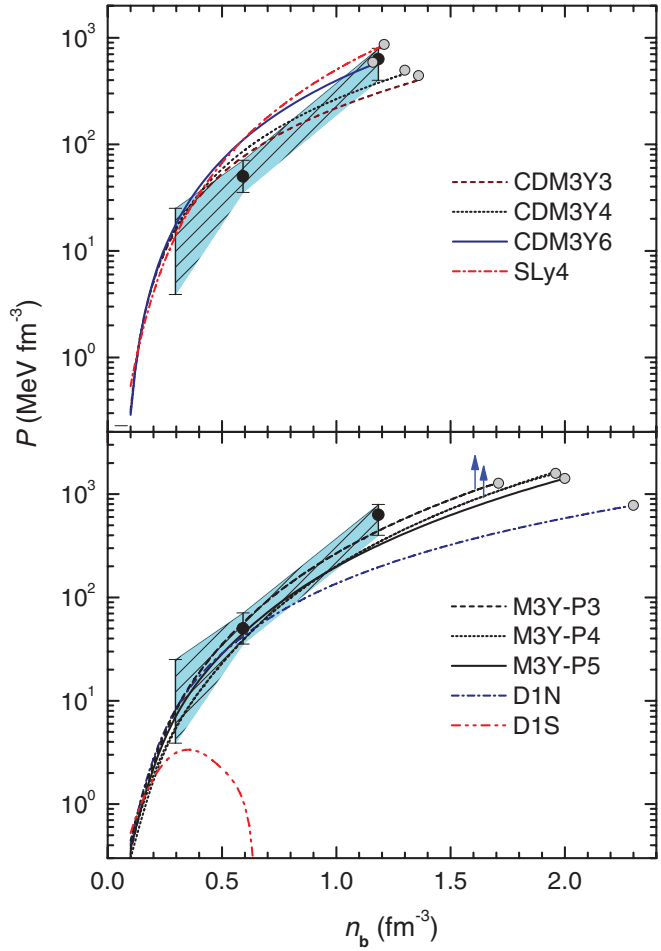

FIG. 7. (Color online) The pressure inside the NS matter obtained with the in-medium NN interactions that give *stiff* (upper panel) and *soft* (lower panel) behaviors of $S(n_b)$, in comparison with the empirical data points deduced from the astronomical observation of neutron stars [58]. The shaded band shows the uncertainties associated with the data determination. The circles are P values calculated at the corresponding maximum central densities given by the TOV equations and the vertical arrows indicate the baryon densities above which the NS matter predicted by the M3Y-P3 and M3Y-P4 interactions becomes superluminal (see Fig. 13).

shaded contours. One can see that all mass-radius curves lie well below the limit allowed by the general relativity [63] and go through or very closely nearby the empirical contours spanned by the data, excepting the curve given by the D1N version of the Gogny interaction that lies well below the data. We note that the same EOS for the NS crust (generated in the CLDM using model parameters determined by the SLy4 interaction [5,30]) has been used in the input of the TOV equations (11). Therefore, the difference found between the mass-radius curves shown in Fig. 8 is entirely due to the different choices of the in-medium NN interaction used to generate the EOS of the NS core. The maximum gravitational masses M_G given by the EOS's under study are plotted in Fig. 8 as solid circles and they agree more or less with the recent data. While all the stiff-type interactions give the corresponding NS radius R_G quite close to the empirical range around 10 km, the

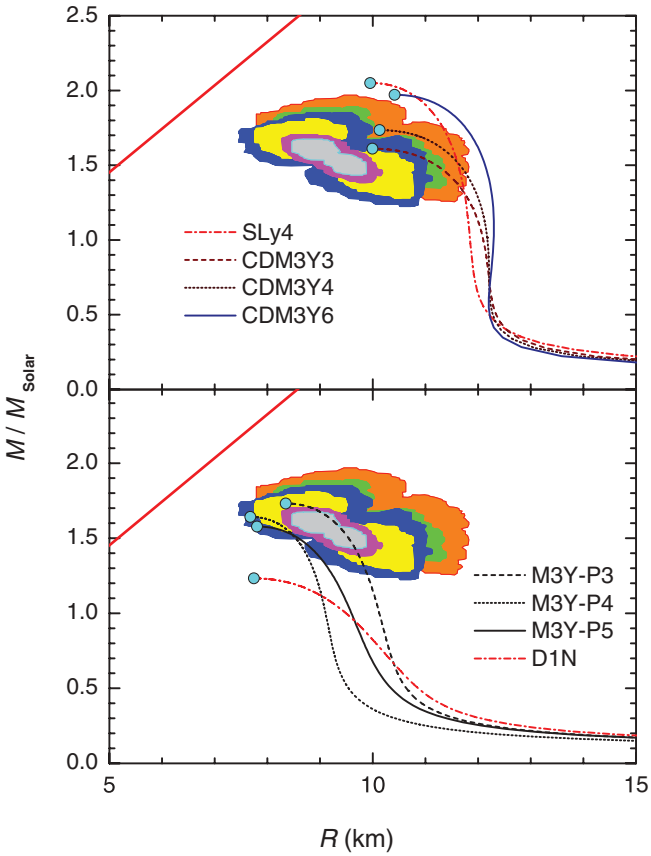

FIG. 8. (Color online) The NS gravitational mass versus its radius obtained with the EOS's given by the stiff-type (upper panel) and soft-type (lower panel) in-medium NN interactions, in comparison with the empirical data (shaded contours) deduced by Özel *et al.* [58] from recent astronomical observations of neutron stars. The circles are values calculated at the maximum central densities. The thick solid (red) line is the limit allowed by the general relativity [63].

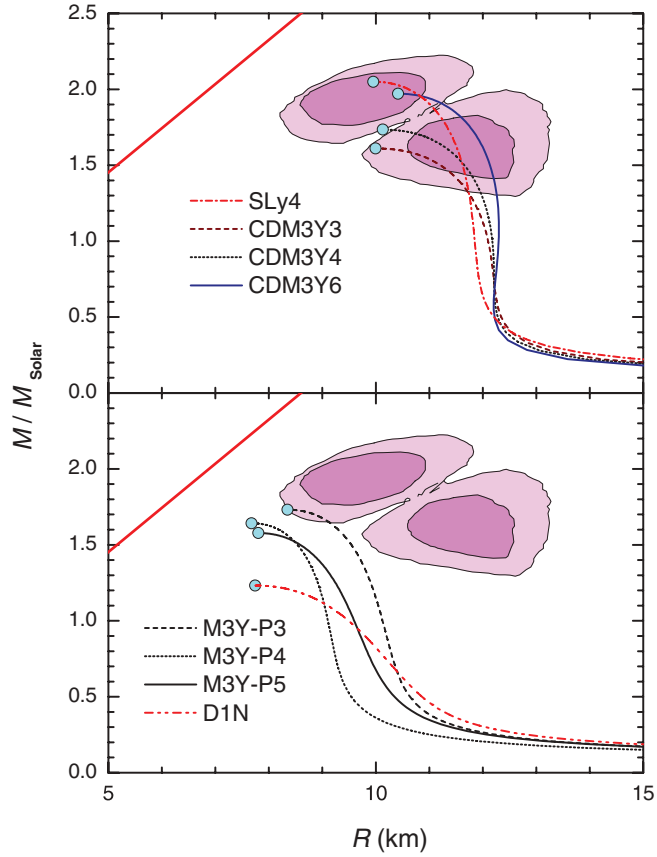

FIG. 9. (Color online) The same as Fig. 8, but in comparison with the empirical data (shaded contours) deduced by Steiner *et al.* [59] from the observation of the x-ray burster 4U 1608-52.

M_G values given by the Sly4 and CDM3Y6 interactions are slightly higher than the observed masses, close to about twice the solar mass ($M_\odot$). We note, however, that the NS matter in the present study has been assumed to consist only of baryons, electrons, and muons. At high baryon densities ($n_b \gtrsim 3n_0$) the hyperons are expected to appear and the maximum NS mass becomes then smaller [6,63]. In this case, the nucleon matter generated with the Sly4 or CDM3Y6 interactions seems well suitable for the description of the baryon component of the NS matter, while the inclusion of hyperons might pull the M_G values given by the soft-type M3Y-Pn interaction to values lying below the empirical boundaries shown in Fig. 8 for the maximum NS mass. Moreover, the M_G values around $2M_\odot$ are still allowed by a broad systematics of the measured NS masses [6,59]. For the D1N interaction, the M_G value is still within the broad range of the measured NS masses [6] but the radius R_G is rather small, almost 1 km smaller than the minimum limit for R versus M: $R \gtrsim 3.6 + 3.9(M/M_\odot)$ km [6].

We stress again that the existing data for the NS mass still allow a wide range for the realistic M_G value, from the lowest value of 1.25 $M_\odot$ [66] up to around 2 $M_\odot$ [6,59], and the comparison of the predicted results *for both mass and radius* is, therefore, vital in testing different EOS's of the NS matter. As another example, we also compared in Fig. 9 the results predicted by different EOS's with the mass-radius data deduced by Steiner *et al.* [59] from the observation of the Type-I x-ray burster 4U 1608-52. One can see that the results given by the EOS's obtained with the stiff-type interactions agree nicely with the empirical data, while those given by the soft-type interactions clearly disagree with the considered mass-radius data. Because the TOV equations are deduced from the Einstein's general relativistic equations for a *gravitationally* bound star in the hydrostatic equilibrium, the results shown in Fig. 8 indicate that the EOS's given by both groups of the in-medium NN interactions (excepting perhaps the D1N interaction) can describe reasonably the empirical mass-radius data deduced by Özel *et al.* [58], despite drastically different proton fractions predicted for the NS matter at supranuclear densities that lead to very different scenarios for the NS cooling as discussed in the previous section. Nonetheless, the comparison of our results with the mass-radius data deduced by Steiner *et al.* [59] seems to prefer the stiff-type interactions.

The moment of inertia I of a slowly rotating neutron star has been shown [64] as a good constraint for the EOS of neutron stars and the physics of their interiors. In general,

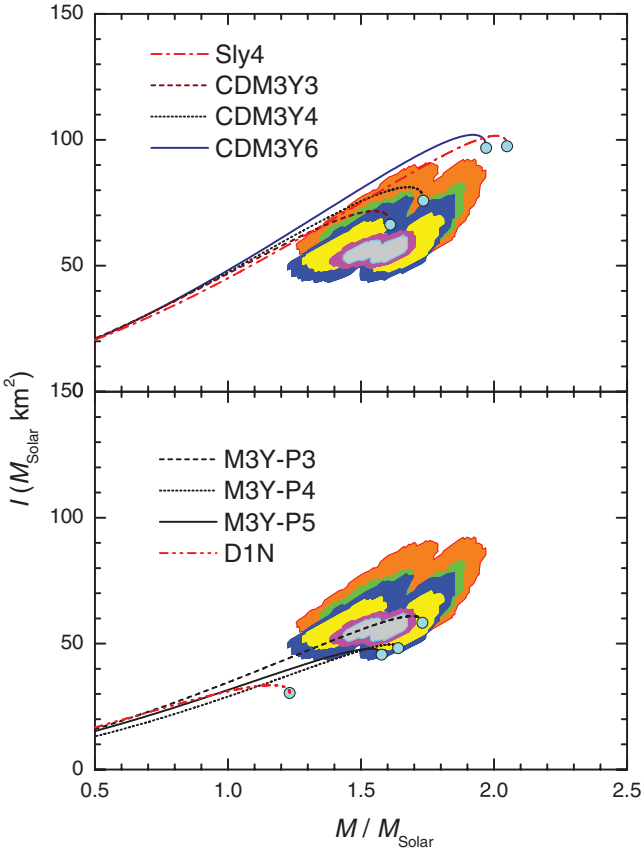

FIG. 10. (Color online) The NS moment of inertia versus its gravitational mass obtained with the EOS's given by the stiff-type (upper panel) and soft-type (lower panel) in-medium NN interactions, in comparison with the empirical data (shaded contours) deduced from the mass-radius data by Özel *et al.* [58] using Eq. (13). The circles are values calculated at the maximum central densities.

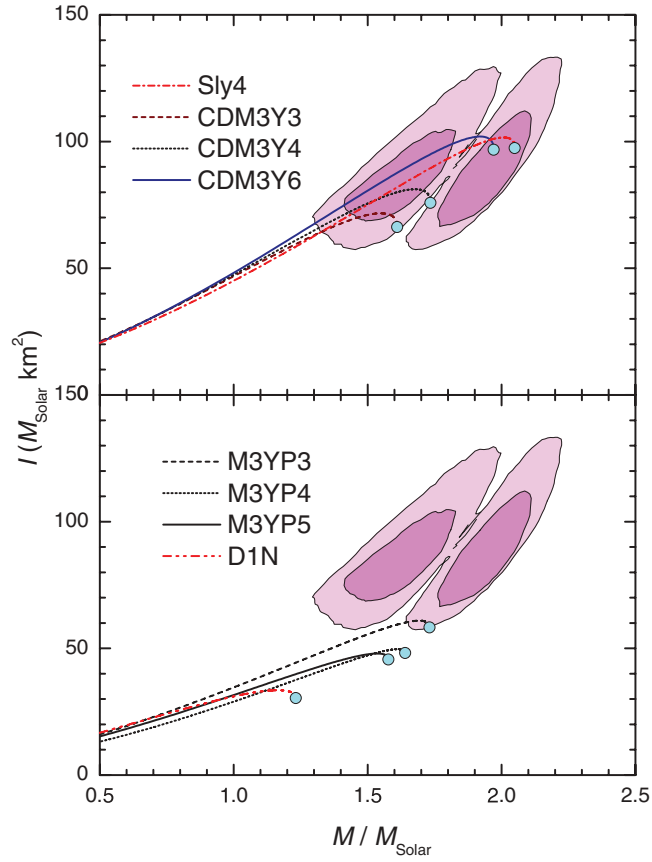

FIG. 11. (Color online) The same as Fig. 10, but in comparison with the empirical data (shaded contours) deduced from the mass-radius data by Steiner *et al.* [59] for the x-ray burster 4U 1608-52 using Eq. (13).

I can be determined from the Einstein field equations for a compact star [65]. It has been shown [64,65] that for slowly rotating neutron stars the expression for I determined from the Einstein field equations can be approximated quite well by the following empirical relation of the NS mass and radius

$$I \approx (0.237 \pm 0.008) M R^2 \times \left[1 + 4.2 \frac{M}{M_\odot}\frac{\text{km}}{R} + 90\left(\frac{M}{M_\odot}\frac{\text{km}}{R}\right)^4\right]. \quad (13)$$

Assuming the validity of relation (13), we have transformed the recent mass-radius data by Özel *et al.* [58] and Steiner *et al.* [59] into the empirical boundaries for realistic values of the moment of inertia. These new empirical "data" for the NS moment of inertia I are plotted in Figs. 10 and 11 by similarly shaded contours as in Figs. 8 and 9, and compared with the results obtained with different EOS's using relation (13). In this way, it is natural to see that the EOS giving the best agreement with the mass-radius data also gives the corresponding I curves agreeing well with the empirical data for the moment of inertia. We conclude from the results shown in Figs. 8 through 11 that the stiff-type NN interactions give a consistently good description to both sets of the empirical data for the NS masses, radii, and moments of inertia.

The main characteristics of the NS configuration determined from the TOV equations (11), using different EOS's, are given in Table I. As noted above, the EOS determined by the D1S version of the Gogny interaction gives *negative* pressure at high baryon densities and violates, therefore, the main constraint for a gravitationally bound star [63] in the hydrostatic equilibrium. As a result, the EOS given by the D1S interaction cannot be used in the TOV equation (11). From Table I one can see that the stiff-type CDM3Y*n* and Sly4 interactions give the maximum gravitational mass $1.6\ M_\odot \lesssim M_G \lesssim 2M_\odot$ and radius $R_G \approx 10$ km that are well within the established empirical boundaries as shown in Figs. 8 and 9. We note that both the *ab initio* APR calculation [50] and microscopic Monte Carlo study [51] have obtained $M_G \gtrsim 2M_\odot$ and the corresponding moment of inertia I_G is, therefore, also somewhat larger than the I_G values given by the stiff-type interactions considered here. The soft-type M3Y-P*n* and, especially, D1N interactions give the M_G and R_G values significantly lower than those given by the stiff-type interactions. Therefore, if hyperons are included at high baryon densities, the M_G and R_G values given by the soft-type interactions can be well below all the existing empirical estimates.

TABLE I. Configuration of a static neutron star given by different NS equations of state: maximum gravitational mass M_G, radius R_G, and moment of inertia I_G; maximum central baryon density n_c, mass density ρ_c, and total pressure P_c; total baryon number A; surface redshift $z_{\rm surf}$; binding energy $E_{\rm bind}$.

EOS	M_G ($M_\odot$)	R_G (km)	n_c (fm^{-3})	ρ_c (10^{15} g/cm^3)	P_c (MeV fm^{-3})	A (10^{57})	$z_{\rm surf}$	$E_{\rm bind}$ (10^{59} MeV)	I_G ($M_\odot$ km^2)
CDM3Y3	1.61	10.01	1.37	2.97	444.0	2.19	0.381	2.35	66.33
CDM3Y4	1.73	10.13	1.30	2.87	495.4	2.38	0.423	2.77	75.81
CDM3Y6	1.97	10.42	1.17	2.66	596.0	2.76	0.506	3.65	96.78
M3Y-P3	1.73	8.36	1.71	4.10	1297.0	2.46	0.606	3.52	58.33
M3Y-P4	1.64	7.72	1.96	4.72	1588.0	2.35	0.640	3.55	48.10
M3Y-P5	1.58	7.81	2.00	4.78	1420.0	2.22	0.576	3.01	45.55
D1N	1.23	7.75	2.36	5.24	819.9	1.65	0.373	1.59	30.28
Sly4	2.05	9.96	1.21	2.86	860.4	2.91	0.590	4.23	97.52
CDM3Y3s	1.13	9.36	1.61	3.26	261.1	1.47	0.246	1.12	35.62
CDM3Y4s	1.21	9.51	1.54	3.15	275.7	1.60	0.267	1.32	40.56
CDM3Y6s	1.42	9.74	1.46	3.06	340.4	1.90	0.326	1.86	52.78

From solutions of the TOV equations at a given radius R, the total baryon mass enclosed within the sphere of radius R can be determined as $M_b(R) = m_N a(R)$, where m_N is the nucleon mass and the total baryon number $a(R)$ is given by Eq. (12). As a result, the $M_b(R)$ values are closely correlated with the corresponding gravitational mass $M(R)$, and difference between these two masses depends upon the compactness of the neutron star. Furthermore, the low-mass part of the dependence of gravitational mass on the total baryon mass $M(M_b)$ can be directly compared with the constraint suggested by Podsiadlowski *et al.* [66]. Namely, in a likely scenario that the massive component of the double pulsar PSR J0737-3059 (the lightest NS observed to date) has been formed by an electron-capture supernova, the total precollapse baryon number of the stellar core (rather precisely known from the model calculations) has a very small loss of material in the subsequent collapse. Therefore, the accurate gravitational mass $M = 1.249 \pm 0.001\ M_\odot$ estimated from the pulsar timing can be used to extract a stringent constraint on the low-mass part of $M(M_b)$, which is plotted as the shaded rectangle in Fig. 12. As discussed also in Ref. [51], a realistic EOS of the NS matter should give $M(M_b)$ curve going through or nearby the shaded box in Fig. 12 to be consistent with the observation of the double pulsar PSR J0737-3059. One can see that the stiff-type NN interactions give $M(M_b)$ curves passing very close to the left corner of the shaded box, while those given by the soft-type interactions clearly underestimate the empirical data. At $M \approx 1.25 M_\odot$, the baryon density ($n_b > 3n_0$) is well above the hyperon threshold and the gravitational mass should become smaller if the hyperons are included [6,63]. This would probably push the $M(M_b)$ curves given by the stiff-type interactions right into the shaded box in Fig. 12. In contrast, there is no physics mechanism that can push the $M(M_b)$ curves given by the soft-type interactions higher up, to be close to the empirical shaded region.

Another important NS observable is the surface redshift of photons emitted from the NS photosphere that is determined as [5]

$$z_{\rm surf} = \left(1 - \frac{r_g}{R}\right)^{-1/2} - 1, \quad \text{where } r_g = \frac{2GM}{c^2} \approx 2.95 \frac{M}{M_\odot}. \tag{14}$$

It is obvious from Eq. (14) that the measurement of $z_{\rm surf}$ is vital for the determination of the mass/radius ratio. At the typical masses around $M \approx 1.5 M_\odot$, the stiff-type CDM3Yn interactions give $z_{\rm surf} \approx 0.30$–$0.35$ while the soft-type M3Y-Pn interactions give $z_{\rm surf} \approx 0.35$–$0.40$, which agree reasonably with the empirical value $z_{\rm surf} \approx 0.35$ deduced from the x-ray

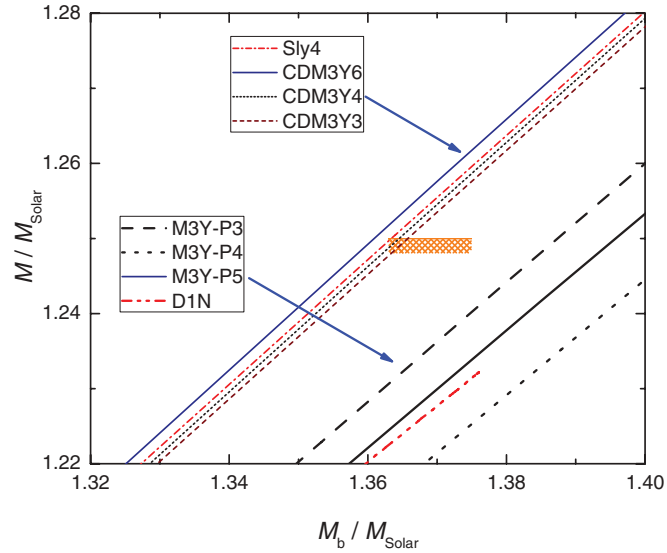

FIG. 12. (Color online) The gravitational mass M given by different EOS's of the NS matter plotted versus the corresponding total baryon mass M_b. The shaded rectangle is the empirical value inferred from observations of the double pulsar PSR J0737-3059 by Podsiadlowski *et al.* [66].

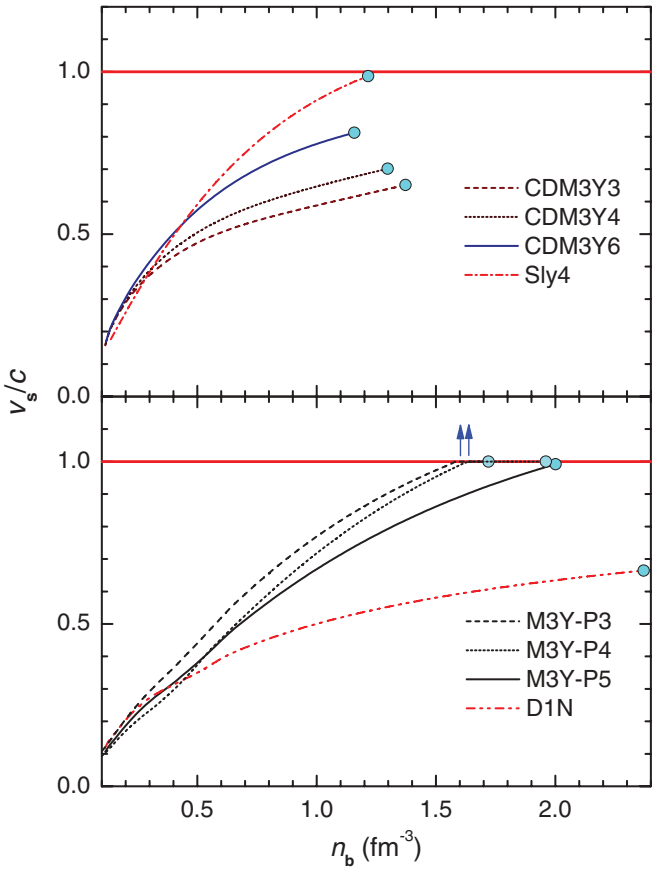

FIG. 13. (Color online) The adiabatic sound velocity versus baryon density obtained with the EOS's given by the stiff-type (upper panel) and soft-type (lower panel) in-medium NN interactions. The thick solid (red) lines are the subluminal limit ($v_s \leqslant c$), and the vertical arrows indicate the baryon densities above which the NS matter predicted by the M3Y-P3 and M3Y-P4 interactions becomes superluminal (see details in the text).

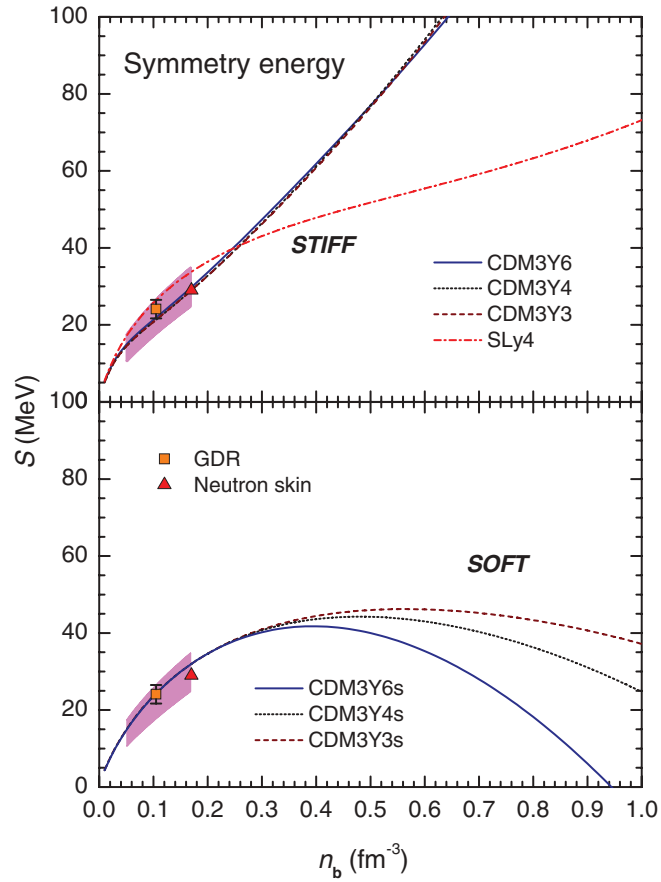

FIG. 14. (Color online) The same as in Fig. 1 but $S(n_b)$ curves in the lower panel were obtained with the soft CDM3Yns interactions.

spectra of the burster EXO 0748-676 [67]. Although the maximum $z_{\rm surf}$ value given by the D1N interaction is close to that empirical data, the maximum NS mass is only around $1.2M_\odot$, and this effect is also showing up in a poor agreement of the D1N results with the mass-radius data as illustrated in Figs. 8 and 10.

For the NS binding energy, we used the standard definition of $E_{\rm bind}$ as the mass defect with respect to an unbound configuration consisting of the same baryon number [5]. Namely, the mass defect with respect to a dispersed configuration of a pressureless cloud of ^{56}Fe dust, with mass per nucleon $m_{\rm Fe}$ = mass of ^{56}Fe atom divided by 56

$$E_{\rm bind} = (Am_{\rm Fe} - M)c^2. \tag{15}$$

At the typical masses around $1.5M_\odot$, all considered interactions give $E_{\rm bind}$ values within the range of $(2 \div 3) \times 10^{59}$ MeV. The exception again is the D1N interaction that gives a weaker binding energy of $E_{\rm bind} \approx 1.6 \times 10^{59}$ MeV with the maximum gravitational mass $M_G \approx 1.2M_\odot$.

Concerning the maximum central pressure, the TOV equations using the EOS's based on the soft-type M3Y-Pn interactions give much too high P_c values (see Table I). The behavior of the central pressure is directly correlated with the central density. In this context, it is of interest to consider the *causality* condition [60] that implies the adiabatic sound velocity in the stellar medium to be *subluminal*, that is,

$$v_s = \sqrt{\frac{dP(\rho)}{d\rho}} \leqslant c, \tag{16}$$

where $P(\rho)$ is the total pressure of the NS matter as a function of the total mass density ρ. We have estimated the sound velocity v_s using the EOS's given by the two groups of the in-medium NN interactions and the results are plotted in Fig. 13. While the soft-type M3Y-Pn interactions give more or less the same v_s values at low densities as those given by the stiff-type CDM3Yn interactions, EOS given by the M3Y-P3 and M3Y-P4 interactions begins to violate the causality condition at $n_b \approx 1.60$ and 1.64 fm^{-3}, respectively. For further use in the TOV equations, we have assumed in these two cases a causal EOS [68] given by $P(\rho) = c^2\rho - \epsilon_C$ at the n_b larger than 1.6 and 1.64 fm^{-3}, respectively, with constant ϵ_C chosen to ensure the continuity of the energy density across the critical densities. The M3Y-P5 interaction is doing better and gives $v_s \approx 0.992c$ at the maximum central density. For the stiff-type Sly4 interaction, we obtained $v_s \approx 0.987c$ at the maximum n_b, and this value indicates a sound velocity closely comparable to

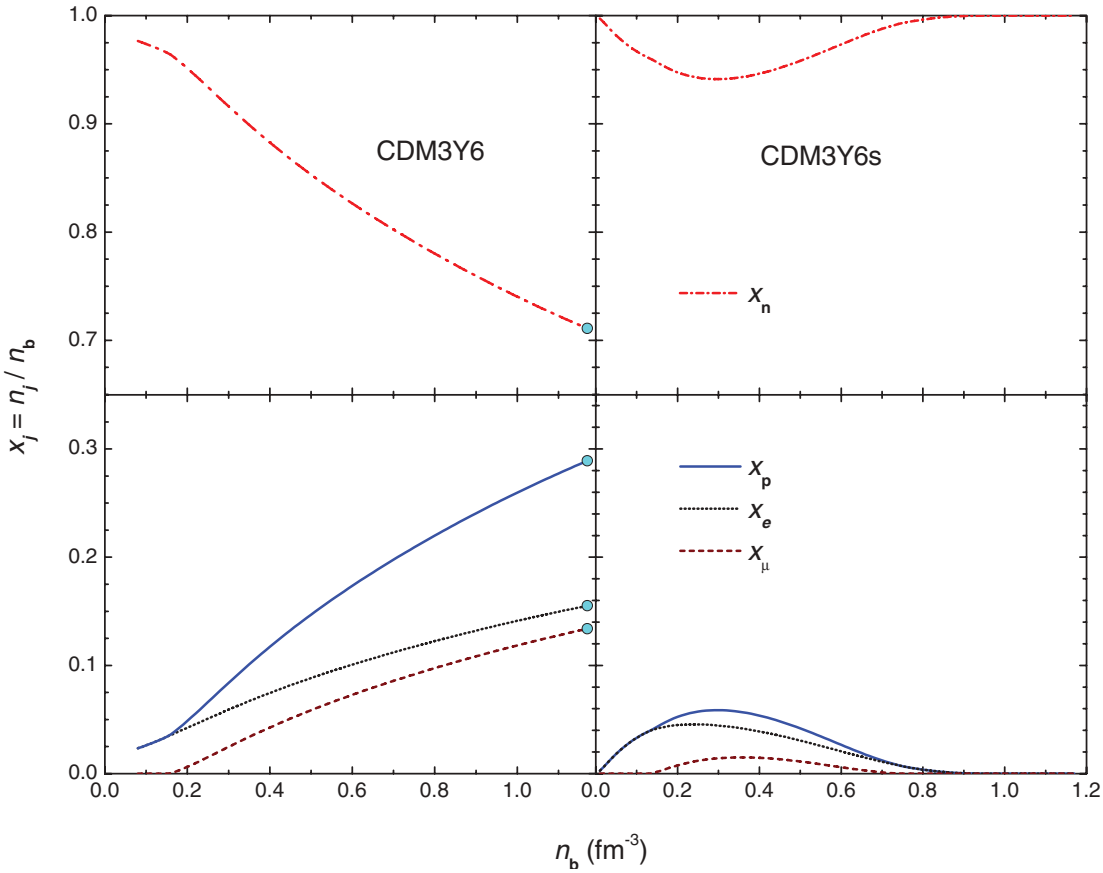

FIG. 15. (Color online) The same as Fig. 4 but using the mean-field potentials given by the CDM3Y6 and CDM3Y6s interactions.

the velocity of light in the dense NS core, as discussed earlier in Ref. [5].

In conclusion, we tested two sets of the in-medium NN interactions in the description of the main properties of neutron-star-based on the TOV equations. We found that all stiff-type interactions are quite realistic in describing the latest empirical constraints for the EOS of the NS matter, pressure, and mass-radius data. In particular, the CDM3Y6 and Sly4 interactions should be the appropriate choice for the future NS studies, when the hyperon presence is taken into account at supranuclear densities. Concerning the soft-type interactions, the EOS's given the M3Y-P3 and M3Y-P4 interactions have been modified at high densities to avoid the violation of the causality condition. Moreover, the overall agreement of the results given by the soft-type interactions with the same empirical data is not as good as that obtained with the stiff-type interactions. It is clear that such effects are caused not only by a drastic difference in the nuclear symmetry energy alone, but also by quite different functional structures of the considered interactions, like, for example, the *zero-range* density-dependent form of the M3Y-P*n* and Gogny interactions versus the *finite-range* form of the CDM3Y*n* interactions.

To explore explicitly the effects caused by the nuclear symmetry energy to the NS properties in this kind of study, one needs to make a similar analysis with the HF energy densities (1) obtained essentially with the same in-medium NN interaction, but using different ansatzs for its isospin dependence so that different behaviors of the symmetry energy $S(n_b)$ can be tested. We present here the results of such a test using the CDM3Y*n* interactions that have the isoscalar (IS) and isovector (IV) parts determined as

$$v_{\mathrm{IS(IV)}}(n_b, s) = F_{\mathrm{IS(IV)}}(n_b) v_{\mathrm{IS(IV)}}(s), \tag{17}$$

where s is the internucleon distance. The radial strengths of the IS and IV interactions $v_{\mathrm{IS(IV)}}(s)$ were kept unchanged, as derived from the M3Y-Paris interaction [10], in terms of three Yukawas (see detailed formulas in Ref. [13]). The isoscalar density dependence $F_{\mathrm{IS}}(n_b)$ was parametrized [14,21] to reproduce the saturation properties of symmetric NM in the HF calculation, while the isovector density dependence $F_{\mathrm{IV}}(n_b)$ was parametrized [15] to reproduce the BHF results for the isospin- and density-dependent nucleon optical potential in the nuclear matter limit [57]. Thus, the stiff behavior of $S(n_b)$ given by the CDM3Y*n* interactions is actually associated with that given by the BHF calculation. In our earlier HF study [13] we have simply assumed the IV density dependence to be the same as that of the IS part, and $S(n_b)$ has then a typical soft behavior that is illustrated in Fig. 14. The same assumption has also been used in the NM studies by Basu *et al.* [16] using the density-dependent version DDM3Y of the M3Y-Reid interaction [9].

To study the effects caused by the stiffness of the symmetry energy, we used in the present work also a soft version of the

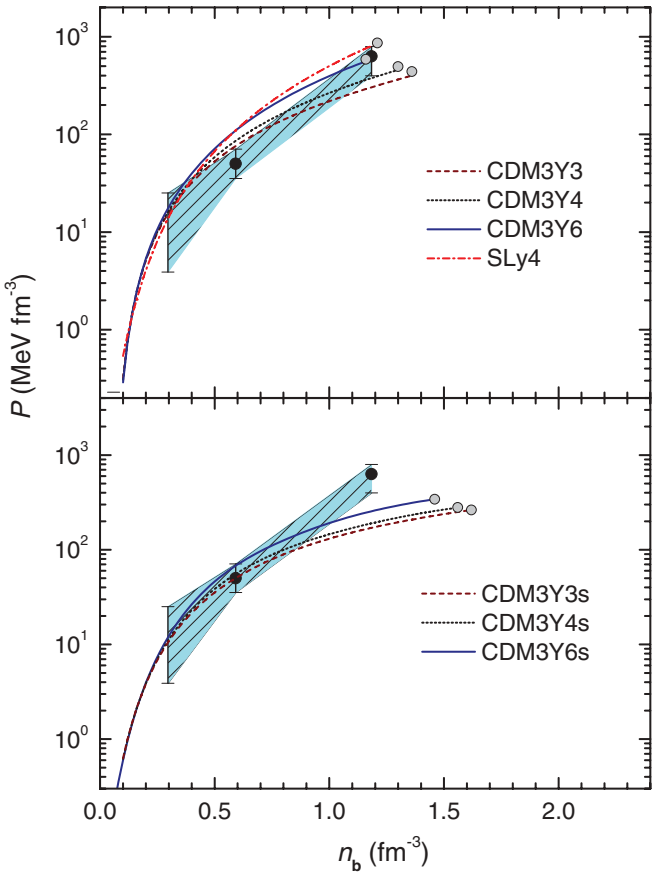

FIG. 16. (Color online) The same as in Fig. 7 but $P(n_b)$ curves in the lower panel were obtained with the soft CDM3Yns interactions.

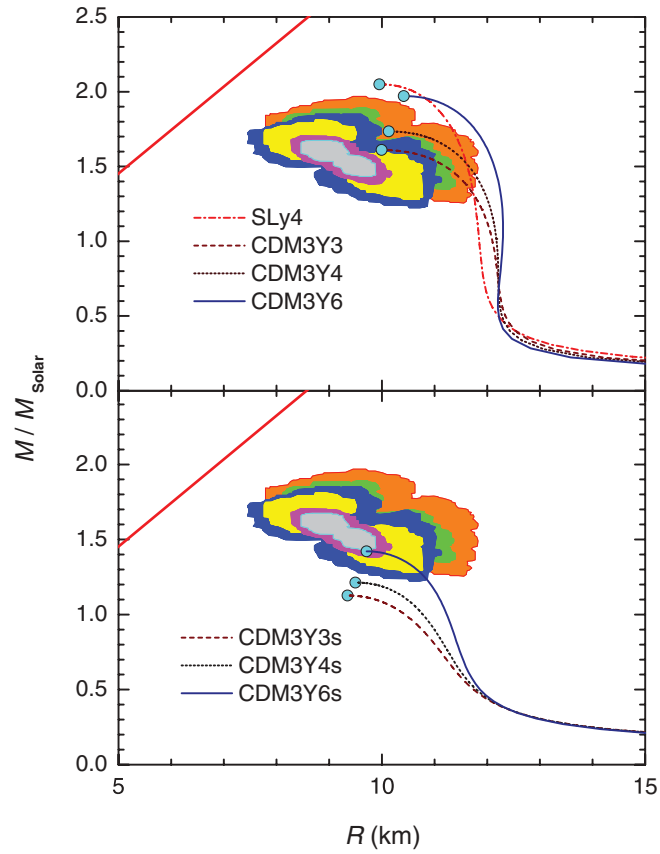

FIG. 17. (Color online) The same as Fig. 8 but mass-radius curves in the lower panel were obtained with the soft CDM3Yns interactions.

CDM3Yn interactions with the IV density dependence taken as $F_{\rm IV}(n_b) = 1.1F_{\rm IS}(n_b)$. The factor of 1.1 was found [20] to give the best fit of the charge exchange ^{6}He$(p,n)^6$Li data as well as a realistic value of the symmetry coefficient $J = S(n_0) \approx 30$ MeV. These soft CDM3Yn interactions (denoted hereafter as the CDM3Yns interactions) give a more moderate *soft* behavior of the symmetry energy compared to the M3Y-Pn interactions (compare Figs. 1 and 14). The soft CDM3Yns interactions were further used to determine the composition of the β-stable NS matter by solving Eqs. (6) and (8), and the fractions $x_j = n_j/n_b$ obtained with the soft CDM3Y6s interaction are compared with those given by the stiff CDM3Y6 version in Fig. 15. As expected, the proton and lepton fractions obtained with the CDM3Y6s interaction are much smaller than those obtained with the stiff CDM3Y6 interaction. The fast decrease of $S(n_b)$ to zero at $n_b \approx 0.8 - 0.9$ fm^{-3} leads also to the disappearance of protons and leptons in the NS matter that soon becomes the β-unstable, pure neutron matter at $n_b \gtrsim 0.9$ fm^{-3}. Like the results obtained with the soft-type M3Y-Pn interactions, the DU scenario of the NS cooling should also be excluded for the NS matter generated with the soft CDM3Yns interactions because x_p can reach only around 5–6% and then decreases quickly to zero at $n_b > 0.8$ fm^{-3}.

The pressures of the NS matter (9) obtained with the two sets of the CDM3Yn interaction are compared with the empirical data in Fig. 16, and one can see that the soft CDM3Yns interactions fail to account for the empirical NS pressure at high densities. This effect is well expected because $P(n_b)$ is determined from the first derivative of the NM energy and the decrease of the NM symmetry energy $S(n_b)$ at high densities leads to a negative contribution of the symmetry term of the NM pressure to the total $P(n_b)$ value. In other words, the EOS's given by the two sets of the CDM3Yn interaction are substantially different at high baryon densities, and this effect is entirely due to the different behaviors of the symmetry energy at high baryon densities.

The mass density ρ and total pressure P of the NS matter (9) obtained with the *soft* CDM3Yns interactions were further used as input of the TOV equations (11), and the obtained NS properties are given in Table I and illustrated in Figs. 17 and 18. The most obvious effect caused by the changing slope of the symmetry energy from *stiff* to *soft* is the reduction of the maximum gravitational mass M_G and radius R_G as illustrated in Fig. 17. The M_G value is changing from 1.6–2 $M_\odot$ to a significantly lower range of 1.1–1.4 $M_\odot$, with a much worse description of the empirical mass-radius data [58,59] as shown in Figs. 17 and 18. Then, if the hyperons are included at high baryon densities, the M_G values given by the soft CDM3Yns interactions can be driven to values lying well below the mass of the lightest NS observed so far ($M = 1.25$ $M_\odot$) [66]. Together with the maximum central pressure P_c, the total baryon number, surface redshift, binding energy, and moment of inertia also become smaller when the EOS of

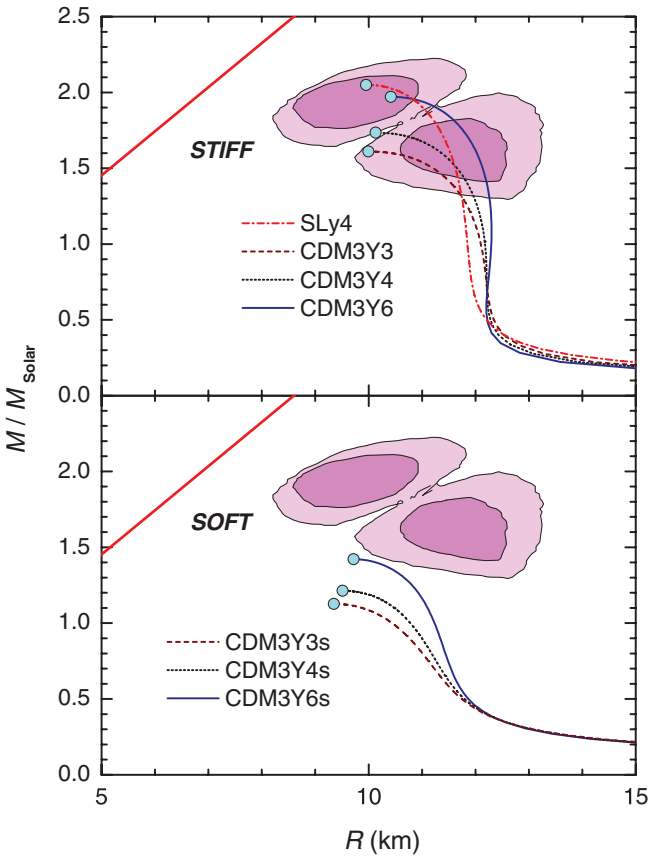

FIG. 18. (Color online) The same as Fig. 9 but mass-radius curves in the lower panel were obtained with the soft CDM3Y*n*s interactions.

the NS core is obtained in the HF calculation using the soft CDM3Y*n*s interactions. It is interesting to note that the EOS's obtained with the soft CDM3Y3*s* and CDM3Y4*s* interactions not only give the NS mass and radius values lying outside the empirical boundaries, but also the surface redshifts $z_{\rm surf}$ clearly in disagreement with the data ($z_{\rm surf} \approx 0.35$) deduced from the x-ray burst spectra of neutron stars [67]. These results together with those obtained with the soft-type M3Y-P*n* and D1N interactions discussed above indicate that a *soft* density dependence of the NM symmetry energy can cause strong deviation of the calculated NS properties from the empirical estimates. Although one still cannot completely rule out the EOS of the NS matter with a *soft* behavior of the symmetry energy based on this discussion, the results shown in Figs. 16 throug 18 clearly favor the *stiff* behavior and confirm again the vital role of the nuclear symmetry energy in the theoretical modeling of the neutron star.

V. SUMMARY

The EOS of the $npe\mu$ matter of the neutron star in β equilibrium was studied in detail using the nuclear mean-field potentials obtained in the HF method with different choices of the effective (in-medium) NN interactions that give two different behaviors of the NM symmetry energy at supranuclear densities (the *soft* and *stiff* scenarios). The fast decrease of the soft NM symmetry energy to zero at $n_b \approx 0.6$–0.7 fm^{-3} results in a drastic decrease of the proton and lepton components in the uniform NS core that then becomes the β-*unstable*, pure neutron matter at $n_b > 0.6$ fm^{-3}. A very small proton fraction in the NS matter given by the soft-type interactions excludes the direct Urca process in the NS cooling, whereas the DU process is well possible for the β-*equilibrated* NS matter predicted by the stiff-type CDM3Y*n* interactions.

The NS pressure obtained with different in-medium NN interactions is compared with the empirical NS pressure deduced from the recent astronomical observation. In general, the EOS given by the soft-type interactions tend to give pressure lower than the empirical values at high densities. In particular, the D1S version of the Gogny interaction gives negative pressure at baryon densities $n_b \gtrsim 2n_0$ and violates, therefore, le Chatelier's principle that ensures the NS stability. The adiabatic sound velocity estimated from the NS pressure given by two versions of the soft-type M3Y-P*n* interaction becomes superluminal at high baryon densities and violates, therefore, the causality condition, and the EOS was corrected by hand in this case for further use in the TOV equations. It seems, therefore, likely that there could be uncertainties in a well-parametrized effective (density-dependent) NN interaction that are not visible at low nuclear densities, and its success in the nuclear structure study is not sufficient to validate its extrapolation to supranuclear densities.

Different EOS's of the NS core supplemented by the Sly4 EOS of the NS crust given by the compressible liquid drop model have been used for the input of the TOV equations to study how different behaviors of the symmetry energy affect the model prediction of the NS properties. The EOS's obtained with the stiff-type interactions were found to give a consistently reasonable description of the empirical data for the NS mass and radius, and to comply well with the causality condition. In comparison with the same empirical NS data, the soft-type interactions were found less successful, especially, the two versions of the famous Gogny interaction certainly need an appropriate modification before they can be used in the TOV equations to study the structure of the neutron star.

The vital role of the NM symmetry energy was demonstrated in our specific test of the CDM3Y*n* interactions, where we found a significant reduction of the maximum gravitational mass M_G and radius R_G away from the empirical boundaries when the slope of the NM symmetry energy was changed from the *stiff* behavior to the *soft* one. It is natural to expect that if hyperons (and other hypothetical constituents like kaons or quark matter) are included at high baryon densities, the M_G and R_G values given by the soft-type interactions can be driven to a region lying well below all existing empirical estimates.

ACKNOWLEDGMENTS

The present research has been supported by the National Foundation for Scientific and Technological Development (NAFOSTED) under Project No. 103.04.07.09. The first two authors gratefully acknowledge the financial support from IPN Orsay and the LIA FVPPL Programme for their short research stays at IPN Orsay in 2010. DTK thanks Betty Tsang for her helpful comments and discussions.

[1] B. A. Li, L. W. Chen, and C. M. Ko, Phys. Rep. **464**, 113 (2008).
[2] H. A. Bethe, Rev. Mod. Phys. **62**, 801 (1990).
[3] K. Summiyoshi and H. Toki, Astrophys. J. **422**, 700 (1994).
[4] K. Summiyoshi, K. Oyamatsu, and H. Toki, Nucl. Phys. A **595**, 327 (1995).
[5] F. Douchin and P. Haensel, Astron. Astrophys. **380**, 151 (2001).
[6] J. M. Lattimer and M. Prakash, Science **304**, 536 (2004); Phys. Rep. **442**, 109 (2007).
[7] T. Klähn *et al.*, Phys. Rev. C **74**, 035802 (2006).
[8] M. Baldo and C. Maieron, J. Phys. G **34**, R243 (2007).
[9] G. Bertsch, J. Borysowicz, H. McManus, and W. G. Love, Nucl. Phys. A **284**, 399 (1977).
[10] N. Anantaraman, H. Toki, and G. F. Bertsch, Nucl. Phys. A **398**, 269 (1983).
[11] D. T. Khoa and W. von Oertzen, Phys. Lett. B **304**, 8 (1993).
[12] D. T. Khoa and W. von Oertzen, Phys. Lett. B **342**, 6 (1995).
[13] D. T. Khoa, W. von Oertzen, and A. A. Ogloblin, Nucl. Phys. A **602**, 98 (1996).
[14] D. T. Khoa, G. R. Satchler, and W. von Oertzen, Phys. Rev. C **56**, 954 (1997).
[15] D. T. Khoa, H. S. Than, and D. C. Cuong, Phys. Rev. C **76**, 014603 (2007).
[16] D. N. Basu, P. R. Chowdhury, and C. Samanta, Nucl. Phys. A **811**, 140 (2008); P. R. Chowdhury, D. N. Basu, and C. Samanta, Phys. Rev. C **80**, 011305(R) (2009).
[17] H. Nakada and M. Sato, Nucl. Phys. A **699**, 511 (2002).
[18] H. Nakada, Phys. Rev. C **68**, 014316 (2003).
[19] H. Nakada, Phys. Rev. C **78**, 054301 (2008); **82**, 029902(E) (2010).
[20] D. T. Khoa and H. S. Than, Phys. Rev. C **71**, 044601 (2005).
[21] D. T. Khoa, W. von Oertzen, H. G. Bohlen, and S. Ohkubo, J. Phys. G **34**, R111 (2007).
[22] N. D. Chien and D. T. Khoa, Phys. Rev. C **79**, 034314 (2009).
[23] H. S. Than, D. T. Khoa, and N. V. Giai, Phys. Rev. C **80**, 064312 (2009).
[24] J. F. Berger, M. Girod, and D. Gogny, Comput. Phys. Commun. **63**, 365 (1991).
[25] F. Chappert, M. Girod, and S. Hilaire, Phys. Lett. B **668**, 420 (2008).
[26] E. Chabanat, P. Bonche, P. Haensel, J. Meyer, and R. Schaeffer, Nucl. Phys. A **635**, 231 (1998).
[27] J. M. Lattimer, C. J. Pethick, M. Prakash, and P. Haensel, Phys. Rev. Lett. **66**, 2701 (1991).
[28] J. M. Lattimer, K. A. Van Riper, M. Prakash, and M. Prakash, Astrophys. J. **425**, 802 (1994).
[29] D. Page, J. M. Lattimer, M. Prakash, and A. W. Steiner, Astrophys. J. Suppl. Ser. **155**, 623 (2004).
[30] F. Douchin, P. Haensel, and J. Meyer, Nucl. Phys. A **665**, 419 (2000).
[31] W. Zuo, I. Bombaci, and U. Lombardo, Phys. Rev. C **60**, 024605 (1999).
[32] M. Brack, C. Guet, and H. B. Håkansson, Phys. Rep. **123**, 276 (1985).
[33] J. M. Pearson and R. C. Nayak, Nucl. Phys. A **668**, 163 (2000).
[34] M. B. Tsang, Y. Zhang, P. Danielewicz, M. Famiano, Z. Li, W. G. Lynch, and A. W. Steiner, Phys. Rev. Lett. **102**, 122701 (2009); M. B. Tsang, Z. Chajecki, D. Coupland, P. Danielewicz, F. Famiano, R. Hodges, M. Kilburn, F. Lu, W. G. Lynch, J. Winkelbauer, M. Youngs, and Y. X. Zhang, Prog. Part. Nucl. Phys. **66**, 400 (2011).
[35] P. Danielewicz, R. Lacey, and W. G. Lynch, Science **298**, 1592 (2002).
[36] A. Ono, P. Danielewicz, W. A. Friedman, W. G. Lynch, and M. B. Tsang, Phys. Rev. C **68**, 051601(R) (2003).
[37] Z. Xiao, B. A. Li, L. W. Chen, G. C. Yong, and M. Zhang, Phys. Rev. Lett. **102**, 062502 (2009).
[38] D. V. Shetty, S. J. Yennello, and G. A. Souliotis, Phys. Rev. C **76**, 024606 (2007).
[39] D. V. Shetty, S. J. Yennello, and G. A. Souliotis, Nucl. Instrum. Methods Phys. Res., Sect. B **261**, 990 (2007).
[40] L. W. Chen, C. M. Ko, and B. A. Li, Phys. Rev. Lett. **94**, 032701 (2005).
[41] P. Danielewicz, Nucl. Phys. A **727**, 233 (2003).
[42] P. Arumugam, B. K. Sharma, P. K. Sahu, S. K. Patra, Tapas Sil, M. Centelles, and X. Viñas, Phys. Lett. B **601**, 51 (2004).
[43] B. G. Todd-Rutel and J. Piekarewicz, Phys. Rev. Lett. **95**, 122501 (2005).
[44] J. Piekarewicz and M. Centelles, Phys. Rev. C **79**, 054311 (2009).
[45] J. Piekarewicz, Phys. Rev. C **76**, 064310 (2007).
[46] M. Centelles, X. Roca-Maza, X. Vinas, and M. Warda, Phys. Rev. Lett. **102**, 122502 (2009).
[47] L. Trippa, G. Colò, and E. Vigezzi, Phys. Rev. C **77**, 061304(R) (2008).
[48] B. A. Brown, Phys. Rev. Lett. **85**, 5296 (2000).
[49] R. J. Furnstahl, Nucl. Phys. A **706**, 85 (2002).
[50] A. Akmal, V. R. Pandharipande, and D. G. Ravenhall, Phys. Rev. C **58**, 1804 (1998).
[51] S. Gandolfi, A. Yu. Illarionov, S. Fantoni, J. C. Miller, F. Pederiva, and K. E. Schmidt, Mon. Not. R. Astron. Soc. **404**, L35 (2010).
[52] V. Baran, M. Colonna, V. Greco, and M. Di Toro, Phys. Rep. **410**, 335 (2005).
[53] J. R. Stone, J. C. Miller, R. Koncewicz, P. D. Stevenson, and M. R. Strayer, Phys. Rev. C **68**, 034324 (2003).
[54] R. B. Wiringa, V. Fiks, and A. Fabrocini, Phys. Rev. C **38**, 1010 (1988).
[55] E. N. E. van Dalen, C. Fuchs, and A. Faessler, Eur. Phys. J. A **31**, 29 (2007).
[56] Z. H. Li, U. Lombardo, H. J. Schulze, W. Zuo, L. W. Chen, and H. R. Ma, Phys. Rev. C **74**, 047304 (2006).
[57] J. P. Jeukenne, A. Lejeune, and C. Mahaux, Phys. Rev. C **16**, 80 (1977).
[58] F. Özel, G. Baym, and T. Güver, Phys. Rev. D **82**, 101301(R) (2010).
[59] A. W. Steiner, J. M. Lattimer, and E. F. Brown, Astrophys. J. **722**, 33 (2010).
[60] I. Bombaci, *Isospin Physics in Heavy Ion Collisions at Intermediate Energies*, edited by B. A. Li and W. U. Schröder (Nova Science, New York, 2001), p. 35.
[61] [http://www.ioffe.ru/astro//NSG/NSEOS/index.html].
[62] G. Shen, C. J. Horowitz, and S. Teige, Phys. Rev. C **83**, 035802 (2011).

[63] N. K. Glendenning, *Compact Stars: Nuclear Physics, Particle Physics and General Relativity* (Springer, New York, 2000).
[64] J. M. Lattimer and B. F. Schutz, Astrophys. J. **629**, 979 (2005).
[65] A. Worley, P. G. Krastev, and B. A. Li, Astrophys. J. **685**, 390 (2008).
[66] Ph. Podsiadlowski, J. D. M. Dewi, P. Lesaffre, J. C. Miller, W. G. Newton, and J. R. Stone, Mon. Not. R. Astron. Soc. **361**, 1243 (2005).
[67] J. Cottam, F. Paerls, and M. Mendez, Nature (London) **420**, 51 (2002).
[68] C. E. Rhoades Jr. and R. Ruffini, Phys. Rev. Lett. **32**, 324 (1974).